

# Mechanism of a 'Schottky-barrier-limited' $\text{Bi}_2\text{Sr}_2\text{CaCu}_2\text{O}_{8+x}$ -based sensor for CO and NO

X.J. Huang <sup>a,1</sup>, J. Schoonman <sup>a</sup>, L.Q. Chen <sup>b</sup>

<sup>a</sup> *Laboratory for Inorganic Chemistry, Julianalaan 136, 2628 BL Delft, Netherlands*

<sup>b</sup> *Institute of Physics, Academia Sinica, PO Box 603, Beijing 100080, China*

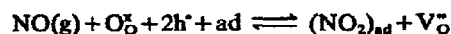
Received 7 September 1993; in revised form 13 June 1994; accepted 19 July 1994

## Abstract

A Taguchi-type sensor with a porous polycrystalline  $\text{Bi}_2\text{Sr}_2\text{CaCu}_2\text{O}_{8+x}$  (BSCCO) film as the active element has been developed. The electrical conductance of the film is 'Schottky-barrier limited'. Its resistivity has been measured as a function of temperature in different CO/air and  $\text{NO}_x$ /air gas mixtures. The power law that is valid for most Taguchi-type sensors is not suitable for fitting the experimental data. The linear relation between  $\ln \ln S + \ln S$  (where  $S$  is the sensitivity of the sensor) and  $\ln P$  (where  $P$  is the partial pressure of the gas in air) is interpreted using a 'Schottky-barrier-limited' model. In this model, the lattice oxygen in the surface layer of this material participates in the sensing reaction. The adsorption of reducing gases decreases the concentration of electron holes in the surface layer. The increase in resistivity is attributed to the rise in height of the Schottky barrier between the primary particles resulting from the lower concentration of the charge carriers. The sensing reaction for CO is proposed to be



and that for NO



The model fits the experimental data for CO sensing, and satisfactorily fits the data for NO sensing at high temperatures. The sensitivity to  $\text{NO}_2$  is ascribed to the NO formed by its decomposition.

**Keywords:** BSCCO; Carbon monoxide sensor; Nitrogen oxide sensor; Schottky barrier

## 1. Introduction

Semiconductor-type sensors are structurally simple and generally inexpensive, because their essential part usually comprises a screen-printed thick film or an evaporated (or sputtered) thin film of semiconducting compounds on a ceramic substrate. The detection of a specific kind of gas or gases is based on the fact that adsorption and decomposition of gases and generation/annihilation can bring about a significant change in the electrical conductivity of the semiconductor.

In order to characterize fully the response of semiconducting gas sensors, several models to interpret the experimental data have been reported [1–3].

Usually, n-type materials like  $\text{SnO}_2$  are employed for reducing gases. For a 'Schottky-barrier-limited' sensor, i.e., assuming the conductivity is limited by barriers between the grains, the barrier potential is described in terms of the adsorption of  $\text{O}_2$  species. The reducing gas R removes adsorbed oxygen from the surface via a catalytic reaction  $\text{R} + \text{O}_{2\text{surf}} \rightarrow \text{product}$ . This model can explain the power response behaviour of  $\text{O}_2$ :  $S \propto P_{\text{O}_2}^{-\beta}$  ( $\beta = 0.25\text{--}0.5$ ), and of reducing gases:  $S \propto P_{\text{O}_2}^{-\beta} (1 + K_i P_i)^\beta$  ( $\beta = 0\text{--}1$ ). Here  $S$  denotes the sensitivity of the sensor to a reducing gas,  $K_i$  is an adsorption constant and  $P_i$  denotes the partial pressure of the reducing gases.

Hardly any work has been done on p-type materials, for which it is unlikely that the reducing gas will react only with the adsorbed oxygen on the surface. It may react with lattice oxygen in the surface layer.

<sup>1</sup> Present address: Group for Sensors and Solid-State Ionics, Faculty of Technology, Christian-Albrechts University, Kaiserstrasse 2, D-24143 Kiel, Germany.

Recently, it has been shown that  $\text{Bi}_2\text{Sr}_2\text{CaCu}_2\text{O}_{8+x}$  (BSCCO) is a suitable material for a Taguchi-type NO sensor with interesting sensitivity to NO, and selectivity against CO and  $\text{CO}_2$  [4]. Attempts to improve the sensitivity can be most effective if the sensing mechanism of such devices is fully understood. According to the qualitative results in Ref. [5], NO is assumed to act as a reducing gas like CO under the testing conditions. The removal of lattice oxygen from the surface layer via oxidation of NO seems to be the likely sensing reaction.

In this work, a sensor with a porous thick film of BSCCO is studied. The sensitivities to  $\text{NO}_x$  and CO are measured at different temperatures for different partial pressures. The CO-sensing mechanism has been studied extensively. A comprehensive model is developed. The experimental data are interpreted according to this model. Deviations of the experimental results from the theoretically predicted curves are discussed.

## 2. Outline of the model

### 2.1. Conductivity mechanism

The electronic structure of BSCCO has been investigated by several researchers [6–12] using photoemission or theoretical calculations. BSCCO exhibits metallic conductivity. Band bending occurs due to the net charge in the surface layer. But the experimental data reveal that the resistivity of poorly sintered porous pellets or films decreases with increasing temperature. According to Chang et al. [13], one can speculate that even high-quality cleaved surfaces suffer from loss of oxygen, deviating from the stoichiometry required for high- $T_c$  materials. Watanabe et al. [14] found that the resistivity of the BSCCO film increase when oxygen ions are removed from an as-fabricated film, and decreases when oxygen ions are injected into the film, which has a high initial resistivity due to removal of oxygen ions. It can be assumed that donor levels are being introduced into the semiconducting band gap by oxygen removal. We assume these porous pellets or films have a metallic core with an outer layer of p-conducting cuprous oxides.

A defect model has been used to interpret the relation between the resistivity and the oxygen partial pressure of  $\text{YBa}_2\text{Cu}_3\text{O}_{7-\delta}$  [15–17]. It has been considered that all excess oxygen is present as interstitial defects, and that all excess oxygens are removed from the structure when it is further reduced.

The oxygen incorporation reaction is written as



where  $\text{O}_{\text{O}}^{\times}$  represents the lattice oxygens and  $\text{V}_{\text{O}}^-$  the oxygen-ion vacancies.

Previous studies [18,19] revealed the charge carrier in this material to be an electron hole at room temperature. In addition, the existence of  $\text{Cu}^{3+}$  in the Bi-based 2212-phase has been identified by cyclic voltammetry, Coulometric determination and by a combination of a volumetric measurement technique and iodometric titration [20–22]. If the reduction of oxygen is associated with  $\text{Cu}^{3+}$ , then the reduction reaction can be written as



### 2.2. The behaviour of porous active layers

In the present study, the sensor material is polycrystalline  $\text{Bi}_2\text{Sr}_2\text{CaCu}_2\text{O}_{8+x}$  with a porous structure, and thus offers a high surface area to the atmosphere. Usually, its thickness is much greater than  $1 \mu\text{m}$ . In considering the mechanism of conduction of such porous materials, it is necessary to take account of the structural inhomogeneity, which involves low-resistance cores of crystallites, covered with a high-resistance surface region or grain boundary, at the contact points of different particles.

Fig. 1 shows a poorly sintered sample with ‘Schottky-barrier-limited’ contacts. In the core of the two particles the electrical behaviour is ohmic, and at the point of contact a Schottky barrier forms, arising from charges trapped in the surface states. Fig. 2 shows the equivalent circuit. In this case, the conductivity will be limited by charge transport across the barrier, while its temperature dependence is given by

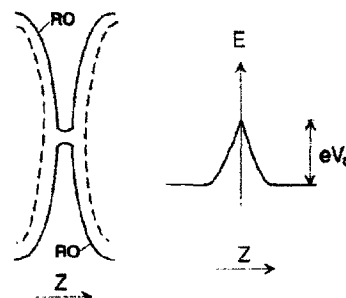


Fig. 1. Schematic of a ‘Schottky-barrier-limited’ contact:  $eV_s$ , the band bending; RO, the chemisorbed species.

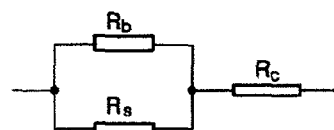


Fig. 2. Equivalent circuit of the sensor:  $R_b$ , bulk resistance;  $R_s$ , surface resistance;  $R_c$ , contact resistance between grains.

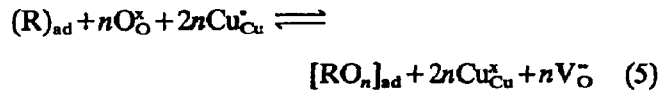
$$\sigma \approx \sigma_0 \exp(-eV_s/kT) \quad (3)$$

with  $\sigma_0$  the pre-exponential factor.

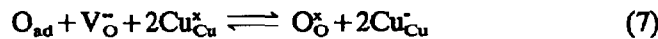
The activation energy for conduction is  $eV_s$ . It will be directly affected by the charge and fractional coverage of the surface species, and, hence, it will be a function of the composition of the gaseous atmosphere.

### 2.3. Model for sensing reducing gases on BSCCO

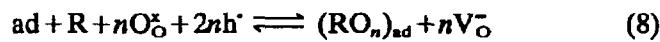
BSCCO exhibits p-type conductivity, and, therefore, chemisorption of reducing gases must lead to an increase in the electrical resistance of the oxide, as observed [4]. A possible mechanism for sensing reducing gas R on BiSCCO can be presented as follows:



with ad denotes a free surface site and  $RO_n$  is the oxidizing product of R. The desorption of  $RO_n$  is followed by adsorption of oxygen,



Eqs. (4), (5) and (7) can be in equilibrium. The overall process can be represented by



Its overall equilibrium constant is written as

$$K = \frac{[(RO_n)_{ad}][V_{\text{O}}^{\times}]^n}{[h^{\cdot}]^{2n}[O_{\text{O}}^{\times}]^n P_R} \quad (9)$$

In the next sections we shall use Eq. (9) to explain the electrical conductivity dependencies on temperature, oxygen content and adspecies concentrations. Therefore, we shall discuss several approximations, such as conductivity being determined by surface traps and Schottky barriers.

The conduction in this case is considered as charge transport across a surface barrier and can be expressed by Eq. (3).

The generation of holes can be considered as an activated process:

$$[h^{\cdot}] = N_A \exp(-E_A/kT) \quad (10)$$

where  $E_A$  is the energy difference between the acceptor level and valence band. The energy difference between the desorbed and adsorbed states of species R is  $E_s - eV_s$  [2]. The equilibrium constant  $K_c$  of chemisorption can be expressed as

$$K_c = \exp[(E_s - eV_s)/kT] \quad (11)$$

Here  $E_s$  denotes the energy level of a surface state evoked by the adsorption of R as a donor, and  $V_s$  the barrier height.

From Eqs. (9), (10) and (11), and using  $K = K_c$ , the adsorbed surface concentration of species R,  $[(RO_n)_{ad}]$  can be expressed as

$$[(RO_n)_{ad}] = N_A^{2n} [O_{\text{O}}^{\times}]^n [V_{\text{O}}^{\times}]^{-n} P_R \times \exp\left(\frac{2nE_A + E_s - eV_s}{kT}\right) \quad (12)$$

The excess charge within the surface layer is approximately

$$\Delta Q_s = 2nN_s [(RO_n)_{ad}] \quad (13)$$

with  $N_s$  the number of acceptor states that can be ionized per unit volume, and assuming that  $[O_{\text{O}}^{\times}]$  (concentration of lattice oxygens) and  $[V_{\text{O}}^{\times}]$  (concentration of oxygen-ion vacancies) are almost constant.

The sensitivity  $S$  is determined as

$$S = \sigma_{\text{air}}/\sigma = \exp(e\Delta V_s/kT) \quad (14)$$

where  $\sigma$  denotes the conductivity in the mixture of air and R, and  $\sigma_{\text{air}}$  denotes the conductivity in air as a reference.

$eV_s$  can be calculated by [2]

$$eV_s = Q_s^2/2\epsilon\epsilon_0 N_A \quad (15)$$

The band bending  $e\Delta V_s$  can be written as

$$e\Delta V_s = [(Q_s + \Delta Q_s)^2 - Q_s^2]/2\epsilon\epsilon_0 N_A \quad (16)$$

Fig. 3 shows the relation between the change in the band bending  $e\Delta V_s$  and  $S$  as calculated from Eq. (14). Since the sensitivity of the sample is less than two, the value of  $e\Delta V_s$  is much lower than  $eV_s^0$  in air, as can be read in Fig. 3. The value of  $eV_s^0$  is 0.08 eV and will be calculated later. Therefore, the value of  $\Delta Q_s$  in Eq. (16) is much less than that of  $Q_s$ . Then Eq. (16) can be rewritten as

$$e\Delta V_s = Q_s \Delta Q_s / \epsilon\epsilon_0 N_A \quad (17)$$

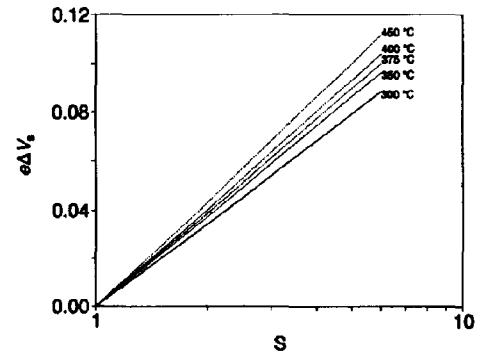


Fig. 3. The calculated relation between  $e\Delta V_s$  and  $S$  for a sensor with a 'Schottky-barrier-limited' conductance at different temperatures.

Combining Eqs. (12), (13) and (17) gives

$$\frac{e\Delta V_s}{kT} = \frac{2N_s Q_s}{\epsilon\epsilon_0 kT} N_A^{2n-1} [O_O^\times]^n [V_O^\bullet]^{-n} P_R \times \exp\left(\frac{2nE_A + E_s - eV_s^0}{kT}\right) \exp\left(\frac{-e\Delta V_s}{kT}\right) \quad (18)$$

Combining Eqs. (14) and (18) results in

$$\ln(\ln S) + \ln S = C + \ln P_R \quad (19)$$

with

$$C = \ln\left(\frac{2N_s Q_s}{\epsilon\epsilon_0 kT} N_A^{2n-1} [O_O^\times]^n [V_O^\bullet]^{-n}\right) + \frac{2nE_A + E_s - eV_s^0}{kT} \quad (20)$$

From Eq. (19) we can find the relation between the sensitivity and the partial pressure of reducing gases in the case of 'Schottky-barrier-limited' conductance.

### 3. Experimental

The starting material  $\text{Bi}_2\text{Sr}_2\text{CaCu}_2\text{O}_{8+x}$  was prepared from the oxides using a method described before [4]. The thick film was prepared by screen printing the powder on a 20 mm × 10 mm  $\text{Al}_2\text{O}_3$  substrate. Subsequently, the film was annealed at 600 °C in air for 20 h. Its thickness is 50–100 μm. Silver paint was applied on the two ends to improve the electrical contact between the sample and the Pt electrodes. The resistance of the sample is 79 Ω at 350 °C in air. It was measured using a Keithley multimeter and a Kipp & Zonen recorder (BD40). The sample was exposed to different  $\text{NO}_x$ - or  $\text{CO}_x$ -containing ambients in a test cell. The gas mixture ( $\text{CO}_x$  or  $\text{NO}_x$  in Ar, air or  $\text{O}_2$ ) was established using mass-flow controllers. The partial pressure of  $\text{O}_2$  was kept at the value in air. The total gas flow rate used is 200 ml  $\text{min}^{-1}$ . The values of the sensitivity were measured after sufficient equilibration times. Usually, these are of the order of 10–60 min.

### 4. Results and discussion

Fig. 4 shows the temperature dependence of the relative resistivity,  $\rho/\rho(350^\circ\text{C})$ , of a sensor in air.

An activation energy  $\approx 0.08$  eV is obtained, and, therefore, no metallic behaviour is proposed. In fact, a Schottky-barrier-limited behaviour is observed. These barriers arise at the boundaries between the particles, and consequently induce band bending in the surface layer. Cuprous oxide often has an excess of oxygen ions, and the corresponding cation vacancies trap electron holes from the valence bands. It seems plausible

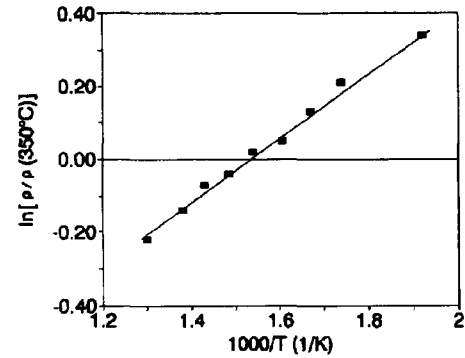


Fig. 4. Temperature dependence of the resistivity in air.

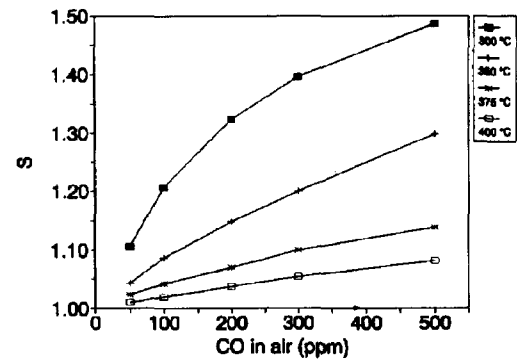


Fig. 5. Temperature dependence of CO sensitivity ( $S$ ).

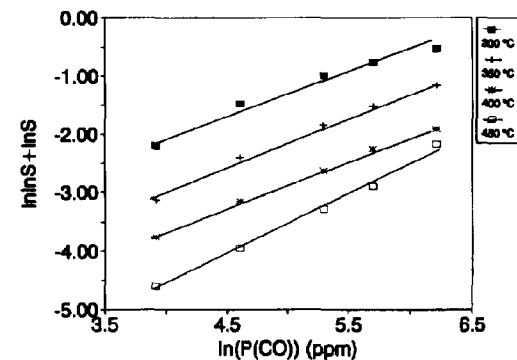


Fig. 6. Plots of  $\ln \ln S_{\text{CO}} + \ln S_{\text{CO}}$  vs.  $\ln P_{\text{CO}}$  at different temperatures.

that for the present materials the bending is caused by removal of lattice oxygen from the surface layer.

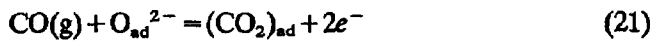
#### 4.1. Sensing behaviour of a BSCCO-based sensor to CO

The temperature and partial-pressure dependencies of the sensitivity of a BSCCO-based sensor to CO are shown in Fig. 5. The curves cannot be fitted to a convenient power relation. Eq. (19) is found to fit these data adequately. Fig. 6 shows a plot of  $\ln \ln S + \ln S$  versus  $\ln P_{\text{CO}}$ . The temperature dependencies of the slopes of the curves in Fig. 6 are listed in Table 1. The average value of the slopes is close to one. Hence, the 'Schottky-barrier-limited' model can be used to describe the sensing behaviour of this sample.

Table 1  
Temperature dependence of the slopes of the plot of  $\ln S_{CO} + \ln S_{CO}$  versus  $\ln P_{CO}$ , and  $\ln S_{NO} + \ln S_{NO}$  versus  $\ln P_{NO}$

Temp. (°C)	300	350	375	400	450
CO	1	1.05	1	1.2	
NO	0.36	0.5	0.54	0.81	1.0

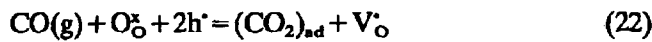
Arakawa et al. and Takaishi [23,24] proposed the following reaction to explain the resistivity change of  $LaCoO_{3-x}$  which they observed:



with  $O_{ad}^{2-}$  the charged surface oxygen species.

However Esser et al. [25] suggested that the surface state should comprise  $CO_2$  associated with  $V_O^\bullet$  on ZnO in the temperature range 500–700 K.

The reaction



is responsible for the conductivity change of the sensor in a CO/air mixture.

Our theoretical consideration uses Langmuir adsorption for R. The Langmuir theory is based on the following assumptions:

(a) Adsorption takes place at separate adsorption centres. Each centre can hold only one gaseous species, and the surface has only one type of adsorption centre characterized by the adsorption heat (the same for all centres), i.e., the same binding energy with respect to a species of a specific type. Such a surface is said to be energy homogeneous.

(b) The adsorbed species do not interact with each other, i.e., the strength with which a given species is coupled to a given centre does not depend upon the type of species at neighbouring centres.

The surface concentration of the adspecies R, i.e.,  $\theta_R$ , for a Langmuir isotherm is defined by

$$\theta_R = \frac{bP_R}{1 + bP_R} \quad (23)$$

with  $b$  the adsorption constant and  $P_R$  the partial pressure of gas R. At low  $P_R$  or low  $b$  values, i.e., if  $bP_R \ll 1$ ,  $\theta_R$  is directly proportional to  $P_R$  (see Fig. 7). However, at high  $P_R$  or high  $b$  values, i.e., if  $bP_R \gg 1$ ,  $\theta_R$  reaches unity (see Fig. 7). The adsorption process is assumed as an activated process; thus, the adsorption constant can be written as

$$b = b^0 \exp(-q/kT) \quad (24)$$

with  $b^0$  the pre-exponential factor determined by the loss or gain of entropy of the adspecies upon adsorption and  $q$  the adsorption heat. From Eq. (24) it is obvious that with increasing temperature,  $b$ , and consequently  $\theta_R$ , decreases.

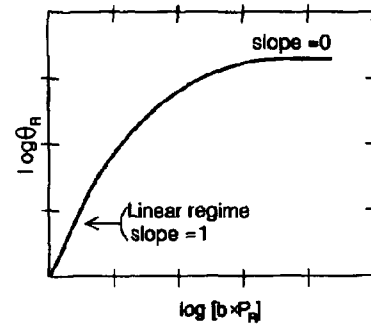


Fig. 7. Theoretical curve of surface concentration of adspecies R vs. the product  $bP_R$ , with  $b$  the adsorption constant and  $P_R$  the partial pressure of gas R as given in Eq. (23).

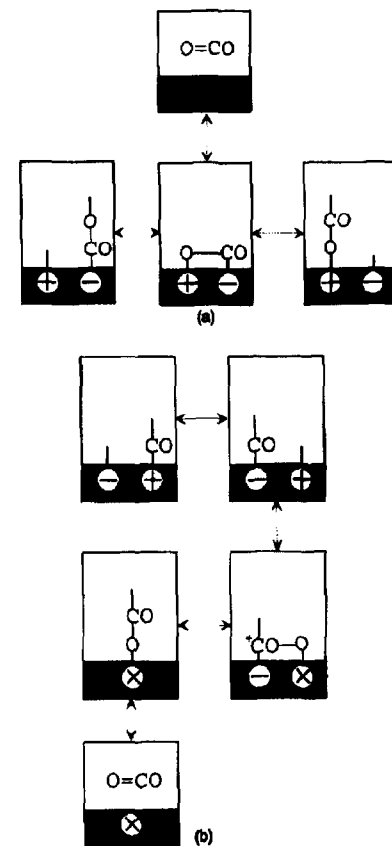


Fig. 8. (a) Schematic outline of the adsorption possibilities of  $CO_2$ , and (b) possible mechanism of the oxidation of CO by a lattice oxygen atom.

At 300 °C, because of the high coverage and high CO concentration, the requirements of Langmuir adsorption cannot be satisfied. Therefore, the slope as shown in Fig. 7 decreases. The other possible reason is that the change of  $[O_O^\bullet]$  and  $[V_O^\bullet]$  can no longer be considered as constant when the coverage of adsorption sites increases. It can be seen that the decrease of  $[O_O^\bullet]$  and increase of  $[V_O^\bullet]$  cause the value of  $C$  in Eq. (19) to decrease (see Eq. (20)).

Fig. 8(a) shows schematically the adsorption possibilities of  $CO_2$  on a solid oxide surface. In 'weak'

chemisorption the CO<sub>2</sub> molecule is bound to the surface state by two bonds. As a result of delocalization of an electron, this form becomes a ‘strong’ donor form, while as a result of delocalization of a hole it would become a ‘strong’ acceptor form. There is no net change in charge as a result of CO<sub>2</sub> adsorption [26]. Therefore, CO<sub>2</sub> has no obvious sensitivity on this material within the framework of the proposed model. Fig. 8(b) shows schematically the oxidation of CO by lattice oxygen ions. Both the oxygen and metal atom can act as adsorption centres for the CO molecules. After the adsorption of molecular CO, surface CO<sup>+</sup> is formed. This then coordinates with a lattice oxygen to form a surface-adsorbed CO<sub>2</sub>. Finally, CO<sub>2</sub> desorbs.

4.2. Sensing behaviour of NO

The temperature and partial-pressure dependencies of the sensitivity of NO of this sensor are shown in Fig. 9. Considering the result of the qualitative analysis [5], the reaction



may cause the conductivity change of the sensor.

Eq. (19) is used to fit the experimental data.

Fig. 10 shows plots of  $\ln \ln S + \ln S$  versus  $\ln P_{\text{NO}}$ . The temperature dependencies of the slopes of the curves are included in Table 1. The values are close to one at high temperatures. At lower temperatures, they deviate from the theoretical value. This deviation

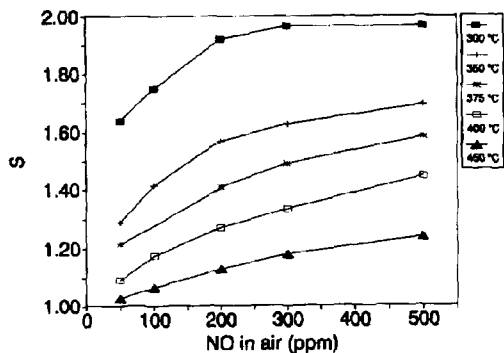


Fig. 9. Temperature dependence of NO sensitivity of Bi<sub>2</sub>Sr<sub>2</sub>CaCu<sub>2</sub>O<sub>8+x</sub>.

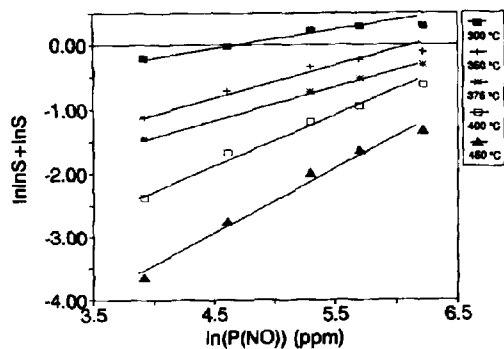


Fig. 10. Plots of  $\ln \ln S_{\text{NO}} + \ln S_{\text{NO}}$  vs.  $\ln P_{\text{NO}}$  at different temperatures.

from the theoretical value of one is probably caused by the high surface concentration of adspecies NO, so it is situated in the non-linear region of the Langmuir isotherm (see Fig. 7).

The possible ways NO<sub>2</sub> can be adsorbed on a solid surface are the same as described for CO<sub>2</sub>. They are ‘weak’ chemisorption, ‘strong’ donor form and ‘strong’ acceptor form, as in CO<sub>2</sub> adsorption on a metal oxide semiconductor. The oxidation of NO by lattice oxygen proceeds like the oxidation of CO. Both the oxygen and metal atom can act as adsorption centres for the NO molecules. On adsorption of NO molecules, surface NO<sup>+</sup> is assumed to be formed, whereas NO<sup>-</sup> is neglected. In Ref. [27] it is assumed that formation of NO<sup>-</sup> is the first reaction step for decomposition of NO. However, NO<sup>+</sup> is formed, and, hence, in contrast to Ref. [27], NO will not decompose. The following reaction step involves coordination with a lattice oxygen ion to form surface NO<sub>2</sub>. Finally, NO<sub>2</sub> desorbs. The selectivity of the thick film prepared by melting the Bi<sub>2</sub>Sr<sub>2</sub>CaCuO<sub>8+x</sub> powder on a polycrystalline Al<sub>2</sub>O<sub>3</sub> substrate to NO against CO is not high. However, it is possible that microstructural and stoichiometry differences will influence the selectivity, and, therefore, further research on this topic is necessary to improve the selectivity of the gas sensor for admixtures of NO<sub>x</sub> and CO<sub>x</sub>. In addition, further work will focus on the influence of the surface and band bending on both the sensitivity and selectivity of the gas sensor.

4.3. Sensing behaviour of NO<sub>2</sub>

Fig. 11 shows the plot of  $\ln \ln S + \ln S$  versus  $P_{\text{NO}_2}$  for different temperatures. The Figure reveals that the sensitivity increases with increasing temperature, i.e., the NO<sub>2</sub> sensitivity at 375 °C is higher than that at 350 °C. This can be understood by the lower NO<sub>2</sub>/NO<sub>x</sub> equilibrium ratio at higher temperature. In other words, the equilibrium concentration of NO increases with temperature. As we can observe from Fig. 11, the relation is almost the same as observed for NO in Fig. 10. Therefore, the assumption in Ref. [5] that the

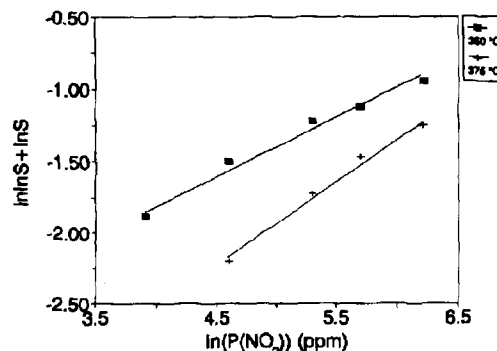
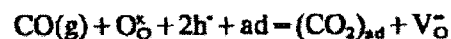


Fig. 11. Plots of  $\ln \ln S_{\text{NO}_2} + \ln S_{\text{NO}_2}$  vs.  $\ln P_{\text{NO}_2}$  at 350 and 375 °C.

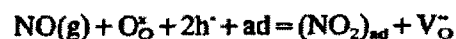
sensitivity to NO<sub>2</sub> is due to the NO formed by decomposition of NO<sub>2</sub> is satisfied.

## 5. Conclusions

The conductance of a porous film of polycrystalline Bi<sub>2</sub>Sr<sub>2</sub>CaCu<sub>2</sub>O<sub>8+x</sub> used as a sensing element in a Taguchi-type gas sensor is 'Schottky-barrier limited'. The power law for most Taguchi-type sensors does not fit suitably the sensitivity–partial gas pressure curves for both CO and NO. A linear relation of  $\ln \ln S + \ln S$  versus  $\ln P$  was observed. This can be interpreted using a 'Schottky-barrier-limited' model. The lattice oxygen in the surface layer of this material is thought to be involved in the sensing reaction. The adsorption of CO or NO decreases the concentration of charge carriers (electron holes) present in the surface layer. The increase of the resistivity is attributed to the increase of the height of the barriers between the grains, which consequently results in a lower concentration of the charge carriers. The possible sensing reaction for CO is proposed to be



and that for NO



The sensitivity to NO<sub>2</sub> is caused by the decomposition of NO.

The reaction mechanism of NO on Bi<sub>2</sub>Sr<sub>2</sub>CaCu<sub>2</sub>O<sub>8+x</sub> is quite complicated. The model in which Eq. (5) is assumed as the sensing reaction can fit the experimental data well at high temperatures. To evaluate the presented relation in accordance with the coverage, the relative position of the Fermi level and reaction routes need to be studied further.

## References

- [1] P.K. Clifford and D.T. Tuma, Characteristics of semiconductor gas sensors, I. Steady state gas response, *Sensors and Actuators*, **3** (1982/83) 233–254.
- [2] J.F. McAleer, P.T. Moseley, J.O.W. Norris and D.E. Williams, Tin dioxide gas sensors, *J. Chem. Soc., Faraday Trans. I*, **83** (1987) 1323–1346.
- [3] T.W. Capehart and S.C. Chang, The interaction of tin oxide films with O<sub>2</sub>, H<sub>2</sub>, NO, and H<sub>2</sub>S, *J. Vac. Sci. Technol.*, **18** (1981) 393–397.
- [4] X.J. Huang, L.Q. Chen and J. Schoonman, High T<sub>c</sub> superconductors as NO<sub>x</sub> and CO<sub>2</sub> sensor materials, *Solid State Ionics*, **57** (1992) 7–10.
- [5] X.J. Huang and J. Schoonman, NO sensing characteristics on Bi<sub>2</sub>Sr<sub>2</sub>CaCu<sub>2</sub>O<sub>8+x</sub> and Bi<sub>2</sub>Sr<sub>2</sub>Cu<sub>1</sub>O<sub>6+x</sub> films, *Solid State Ionics*, to be published.
- [6] H. Krakauer and W.E. Pickett, Effect of bismuth on high-T<sub>c</sub> cuprate superconductors electronic structure of bismuth strontium calcium copper oxide (Bi<sub>2</sub>Sr<sub>2</sub>CaCu<sub>2</sub>O<sub>8</sub>), *Phys. Rev. Lett.*, **60** (1988) 1665–1667.
- [7] R. Manzke, T. Buslaps, R. Claessen, G. Mante and Z.X. Zhao, Partial oxygen density of states of bismuth strontium calcium copper oxide (Bi<sub>2</sub>Sr<sub>2</sub>CaCu<sub>2</sub>O<sub>8</sub>) determined by resonant photoemission, *Solid State Commun.*, **70** (1989) 67–70.
- [8] T.J. Wagener, Y. Hu, Y. Gao, M.B. Jost, J.H. Weaver, N.D. Spencer and K.C. Goretta, Resonant inverse photoemission of bismuth calcium strontium copper oxide (Bi<sub>2</sub>Sr<sub>2</sub>CaCu<sub>2</sub>O<sub>8+x</sub>) and yttrium barium copper oxide (YBa<sub>2</sub>Cu<sub>3</sub>O<sub>7-x</sub>), unoccupied oxygen states, and plasmons, *Phys. Rev.*, **B39** (1989) 2928–2931.
- [9] F. Rochet, A. Balzarotti, M. de Crescenzi, N. Motta, M. Sastry, F. Patella, J. Ferrière, F. Kerhervé, G. Hauchecorne and M. Froment, Electronic properties of laser-deposited bismuth strontium calcium copper oxide (Bi<sub>2</sub>Sr<sub>2</sub>CaCu<sub>2</sub>O<sub>8+x</sub>), *Physica, C* **159** (1989) 447–460.
- [10] S. Kohiki, K. Horochi, A. Adachi, K. Setsune and K. Wasa, Superconducting and copper valence of bismuth strontium calcium copper oxide thin films, *Phys. Rev.*, **B38** (1988) 9201–9204.
- [11] H.M. Meyer III, D.M. Hill, J.H. Weaver, D.L. Nelson and C.F. Gallo, Occupied electronic states of single-crystal bismuth calcium strontium copper oxide (Bi<sub>2</sub>Sr<sub>2</sub>CaCu<sub>2</sub>O<sub>8+x</sub>), *Phys. Rev.*, **B38** (1988) 7144–7147.
- [12] P.A.P. Lindberg, Z.X. Shen, I. Lindu, W.E. Spicer, C.B. Eom and T.H. Geballe, Photoemission study of surface electronic structure of bismuth calcium strontium copper oxide superconductors, *Appl. Phys. Lett.*, **53** (1988) 529–531.
- [13] Y. Chang, N.G. Stoffel, M. Tang, R. Zanoni, M. Onellion, R. Loynt, D.L. Huber, G. Margaritondo, P.A. Morris, W.A. Bonner and J.M. Tarascon, Temperature effects in the near-E<sub>F</sub> electronic structure of Bi<sub>2</sub>Ca<sub>2</sub>Sr<sub>2</sub>Cu<sub>4</sub>O<sub>16+x</sub>, *High T<sub>c</sub> Supercond. Thin Films, Device, Appl.*, 1989, *AIP Conf. Proc.*, Vol. 182, pp. 248–251.
- [14] T. Watanabe, T. Yatabe, H. Yugami and M. Ishigame, Control of oxygen concentration in BSCCO thin films using solid-state electrolytes, *Solid State Ionics* **53–56** (1992) 606–610.
- [15] J. Maier, P. Murugaraj, G. Pfundtner and W. Sitte, Defect chemical investigations of defined barium copper yttrium oxide (YBa<sub>2</sub>Cu<sub>3</sub>O<sub>x</sub>) superconductors, *Ber. Bunsenges. Phys. Chem.*, **93** (1989) 1350–1356.
- [16] M.Y. Su, S.E. Dorris and T.O. Mason, Defect model and transport at high temperature in yttrium barium copper oxide (YBa<sub>2</sub>Cu<sub>3</sub>O<sub>4+x</sub>), *J. Solid State Chem.*, **75** (1988) 381–389.
- [17] J. Molenda, A. Stoklosa and T. Bak, Transport properties of yttrium barium copper oxide (YBa<sub>2</sub>Cu<sub>3</sub>O<sub>7-x</sub>) at high temperatures, *Physica, C* **175** (1991) 555–565.
- [18] A. Mawdsley, H.J. Trodahl, J. Tallon, J. Safati and A.B. Kaiser, Thermoelectric power and electron–photon enhancement in (YBa<sub>2</sub>Cu<sub>3</sub>O<sub>7-x</sub>), *Nature*, **328** (1987) 233–234.
- [19] M. Mukaida, K. Kuroka and S. Miyazawa, Hall coefficient of c-axis oriented bismuth strontium calcium copper oxide 107 K films, *Appl. Phys. Lett.*, **55** (1989) 1129–1131.
- [20] L.Q. Chen, X.J. Huang, T.E. Hui, Y.Z. Huang and J.Q. Bi, The valence of copper in Bi- and Tl-based superconductors, in Z.X. Zhao, G.J. Cui and R.S. Han (eds.), *Progress in High Temperature Superconductor*, Vol. 22, World Scientific, Singapore, 1989, pp. 382–384.
- [21] K. Kuruusu, H. Takami and K. Shintomi, Coulometric determination of the average valence of copper and bismuth in the superconducting bismuth–strontium–calcium–oxygen system, *Analyst*, **114** (1989) 1341–1343.
- [22] H.K. Liu, S.X. Dou, K.H. Song, C.C. Sorrell, K.E. Easterling and W.K. Jones, Cu valence state in superconducting Bi–Pb–Sr–Ca–Cu–O system, *J. Solid State Chem.*, **87** (1990) 289–297.

- [23] T. Arakawa, K. Takada, Y. Tsunemine and J. Shiokawa, CO gas sensitivities of reduced perovskite oxide  $\text{LaCoO}_{3-x}$ , *Sensors and Actuators*, 14 (1988) 215–221.
- [24] T. Takaishi, The ionic adsorption of gases on semiconductor and their catalytic activities, I. Theory of adsorption, *Z. Naturforsch*, A11 (1956) 286–297.
- [25] P. Esser, R. Feierabend and W. Göpel, Comparative study on the reactivity of polycrystalline and single crystal ZnO surface: catalytic oxidation of CO, *Ber. Bunsenges. Phys. Chem.*, 85 (1981) 447–455.
- [26] T. Wolkenstein, *Electronic Processes on Semiconductor Surface During Chemisorption*, Consultants Bureau, New York, 1991.
- [27] C.M. van den Bleek, J.W. Eek, J. Reedijk and P.J. van den Berg, Problems around the reduction of nitrogen oxides in the presence of oxygen, *Int. Chem. Eng. Symp. Ser.*, No. 57 (*Control Sulphur Other Gaseous Emission.*), 1979, R1–R17.